Journal of Alloys and Compounds 509 (2011) 2824–2828

Contents lists available at ScienceDirect

Journal of Alloys and Compounds

journal homepage: www.elsevier.com/locate/jallcom

$SmBaCoCuO_{5+x}$ as cathode material based on GDC electrolyte for intermediate-temperature solid oxide fuel cells

Shiquan Lü [a], Guohui Long [b], Yuan Ji [a,*], Xiangwei Meng [a,c], Hongyuan Zhao [a], Cuicui Sun [a,b]

[a] State Key Laboratory of Superhard Materials, Jilin University, Changchun 130051, PR China
[b] College of Life Sciences, Jilin Agricultural University, Changchun 130118, PR China
[c] Institute of Condensed State Physics, Jilin Normal University, 1301 Haifeng Road, Siping 136000, PR China

ARTICLE INFO

Article history:
Received 11 April 2010
Received in revised form
16 November 2010
Accepted 22 November 2010
Available online 1 December 2010

Keywords:
Solid oxide fuel cells
Cathode
Thermal expansion
Electrochemical performance

ABSTRACT

The performance of $SmBaCoCuO_{5+x}$ (SBCCO) cathode has been investigated for their potential utilization in intermediate-temperature solid oxide fuel cells (IT-SOFCs). The powder X-ray diffraction (XRD), thermal expansion and electrochemical performance on $Ce_{0.9}Gd_{0.1}O_{1.95}$ (GDC) electrolyte are evaluated. XRD results show that there is no chemical reaction between SBCCO cathode and GDC electrolyte when the temperature is below 950 °C. The thermal expansion coefficient (TEC) value of SBCCO is $15.53 \times 10^{-6}\ K^{-1}$, which is ~23% lower than the TEC of the $SmBaCo_2O_{5+x}$ (SBCO) sample. The electrochemical impedance spectra reveals that SBCCO symmetrical half-cells by sintering at 950 °C has the best electrochemical performance and the area specific resistance (ASR) of SBCCO cathode is as low as 0.086 Ω cm² at 800 °C. An electrolyte-supported fuel cell generates good performance with the maximum power density of 517 mW cm^{-2} at 800 °C in H_2. Preliminary results indicate that SBCCO is promising as a cathode for IT-SOFCs.

1. Introduction

A solid oxide fuel cell (SOFC) is an energy-conversion system of great industrial interest because of its high-energy efficiency and environmental advantages [1]. However, for traditional SOFC structures, the necessity for high operating temperatures (800–1000 °C) has resulted in high costs and material compatibility challenges [2]. As a consequence, significant effort has been devoted to the development of intermediate-temperature (IT, 500–800 °C) SOFCs. Unfortunately, one of the main obstacles is that the cathode resistance increases greatly with decreasing temperature [3].

The traditional cathode material $La_{1-x}Sr_xMnO_3$ (LSM) is deemed to be one of the most promising cathode materials for high temperature SOFCs due to its good thermal and chemical stability with yttria-stabilized zirconia (YSZ) [4,5]. However, LSM does not provide adequate performance for IT-SOFCs because of its poor oxide–ion conductivity and lower catalytic activity at intermediate temperature ranges [6,7]. Recently, a new series of perovskite-like compounds $LnBaCo_2O_{5+\delta}$ (Ln=Nd, Sm, Gd, and Y), have drawn much attention due to their ordered structure type [8,9]. This ordered structure is recognized to be able to greatly enhance the diffusivity of oxygen-ion in the bulk of the material by orders of magnitude [10–12], and consequently improves cathode performance. Kim et al. [13] have shown that layered perovskite $SmBaCo_2O_{5+x}$ (SBCO) exhibited high electrical conductivity, reasonable oxide ionic diffusivity and lower polarization resistance, indicating the potential cathodic application for IT-SOFCs. However, these cobalt-based cathodes often suffer some problems like high thermal expansion coefficients (TECs) and high cost of cobalt element [14]. Therefore, more attention should be paid to the B-sites ions. Recently, the $LaBaCuCoO_{5+x}$ cathode based on $BaZr_{0.1}Ce_{0.7}Y_{0.2}O_{3-\delta}$ electrolyte for proton-conducting fuel cells has been reported by Ling et al. [15]. And we know that Nian et al. [16] have also evaluated the performance of layered $SmBaCoCuO_{5+x}$ (SBCCO) as a cathode in proton-conducting fuel cells based on $BaCe_{0.8}Sm_{0.2}O_{3-\delta}$ electrolyte. However, to the best of our knowledge, the performance of SBCCO cathodes in oxygen-ion conducting fuel cells has not been reported to date. In this work, the ceramic powder with a composition of SBCCO synthesized by solid-state reaction is examined as a cathode for IT-SOFCs based on $Ce_{0.9}Gd_{0.1}O_{1.95}$ (GDC) electrolyte.

2. Experimental

2.1. Sample preparation

$SmBaCoCuO_{5+x}$ (SBCCO) oxides were synthesized by conventional solid-state reaction methods. Briefly, Sm_2O_3, $BaCO_3$, Co_2O_3 and CuO were weighed in the stoichiometric proportions of SBCCO, then mixed, ground and pelletized. The mixture was ground thoroughly using an agate pestle and mortar for 2 h, and then pressed into a disk and fired repeatedly at 950, 975, and 1000 °C for 12 h in air, respec-

* Corresponding author. Tel.: +86 431 8566 0418; fax: +86 431 8849 8000.
E-mail address: jiyuan@jlu.edu.cn (Y. Ji).

0925-8388/$ – see front matter © 2010 Elsevier B.V. All rights reserved.
doi:10.1016/j.jallcom.2010.11.128

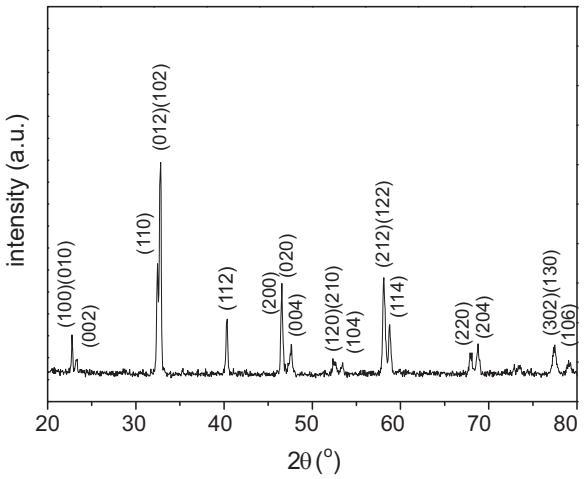

Fig. 1. XRD pattern of $SmBaCoCuO_{5+x}$ (SBCCO) powers.

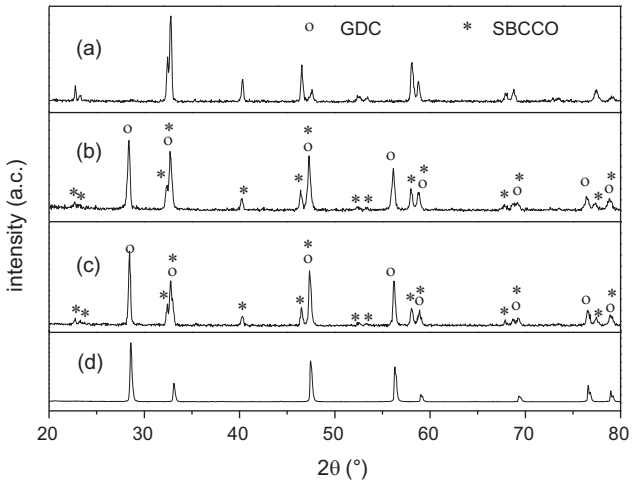

Fig. 2. XRD patterns of (a) SBCCO powders, (b) SBCCO–GDC mixture sintered at 950 °C for 2 h in air, (c) SBCCO–GDC mixture sintered at 800 °C for 20 h in air and (d) $Ce_{0.9}Gd_{0.1}O_{1.95}$ (GDC) powders.

tively. A $Ce_{0.9}Gd_{0.1}O_{1.95}$ (GDC) powder was prepared by the glycine–nitrate process as described elsewhere [17]. Stoichiometric amounts of $Ce(NO_3)_3{\cdot}6H_2O$ and Gd_2O_3 were used as the starting materials. The precursor powders were calcined at 800 °C for 2 h to obtain the GDC powder.

2.2. Fuel cell fabrication

Symmetrical electrochemical cells for impedance studies were prepared using a SBCCO cathode and GDC electrolyte. Fine SBCCO powders were mixed thoroughly with an appropriate organic solvent (10% ethyl cellulose + 90% terpineol) to obtain the cathode slurries. SBCCO cathode slurries were screen printed onto both sides of the GDC electrolytes. After drying, the samples were sintered at 900 °C, 950 °C and 1000 °C for 2 h, respectively.

Electrolyte GDC (thickness of 300 μm) supported fuel cell was fabricated in our experiments. The composite anode consisting of NiO-35GDC (65:35 by weight) and the SBCCO cathode were screen-printed on each side of the GDC disk. After sintering the anode at 1250 °C for 4 h, the SBCCO cathode was sintered at 950 °C for 2 h. Then silver paste was applied to the anode and cathode surfaces to serve as current collectors. A single-cell made in this way was then sealed onto one end of an alumina tube with silver paste.

2.3. Characterization

The phase structure of synthesized powders was characterized with an X-ray diffractometer (XRD, Rigaku-D-Max γA system operating at 12 kW with Cu Kα radiation) with an angle step of 0.02° and a scanning range of 20–80° at room temperature. The electrical conductivity of the sintered sample SBCCO was measured using a van der Pauw method in the temperature range of 100–850 °C. The thermal expansion coefficient (TEC) of the samples was measured using a horizontal push rod dilatometer (Netzsch DIL 402C) with an Al_2O_3 reference in the temperature range from 30 to 850 °C. A JEOL JSM-6480LV scanning electron microscope (SEM) was employed to examine the microstructure of symmetrical half-cells. The electrochemical performance was evaluated by a CHI604C analyzer and ac impedance spectroscopy measurements were carried out under open-circuit conditions from 0.01 Hz to 10^5 Hz with the signal amplitude of 10 mV. The single cell performance was tested under dry H_2 and ambient air at temperatures ranging from 650 to 800 °C in 50 °C intervals.

3. Results and discussion

3.1. Crystal structure and chemical compatibility

Fig. 1 shows an X-ray diffraction pattern of the $SmBaCoCuO_{5+x}$ (SBCCO) oxide sintered at 1000 °C for 12 h in air. It can be seen that SBCCO crystallize in a single phase double-perovskite after sintering at 1000 °C through intermediate grinding and calcining at 950 °C and 975 °C. All the diffraction peaks of SBCCO sample can be indexed with an orthorhombic crystal structure. The results are in agreement with those reported by different groups [9,16,18]. The reaction between electrode and electrolyte is undesirable for the long-term stability of SOFCs. To assess the chemical compatibility between cathode and electrolyte, the phase reaction of SBCCO cathode with GDC electrolyte was examined by XRD analysis. Fig. 2(b) shows the XRD pattern of SBCCO–GDC (50:50 by weight) mixtures sintered at 950 °C for 2 h. For comparison, the patterns of SBCCO and GDC are also shown in the same figure. We can see that all the diffraction peaks could be indexed well based on a physical mixture of SBCCO and GDC phases. It suggests that there are no serious reactions between these two components. Since the cell was operated at 800 °C, the phase of SBCCO–GDC sintered at 800 °C for 20 h were also measured by XRD (Fig. 2(c)). We can see that the SBCCO and GDC still retain their own structures after sintering at 800 °C for 20 h. Preliminary results indicate that SBCCO has a good chemical compatibility with GDC electrolyte, supporting its use as a cathode in IT-SOFCs.

3.2. Electrical conductivity

The Arrhenius plots of $\ln(\sigma T)$ vs. $1/T$ and electrical conductivity vs. temperature in air are shown in Fig. 3. From the Arrhenius plots, three different slopes are obtained in the temperature range 100–350 °C, 400–600 °C and 650–850 °C. The activation energies are calculated from the data of the plots, which are 0.22 ± 0.016 eV, 0.08 ± 0.006 eV and 0.23 ± 0.003 eV for the different temperature ranges. From the temperature dependence of the conductivity, the trend of conductivity change at the temperatures 350–450 °C and 600–650 °C, which is also observed in Refs. [19,20]. The change of the conductivity might be ascribed to the oxygen order–disorder

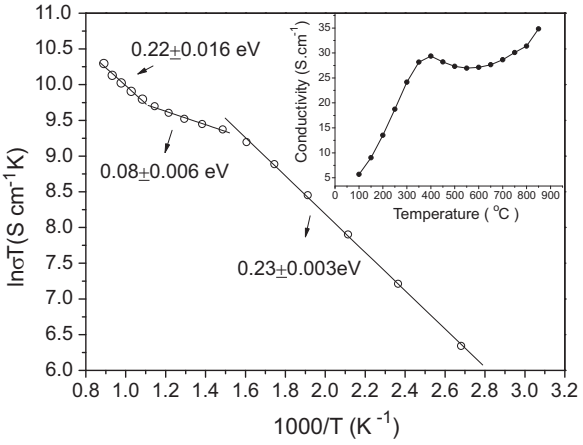

Fig. 3. The Arrhenius plots of $\ln(\sigma T)$ vs. $1/T$ in air and electrical conductivity vs. temperature.

phase transition at the high temperature [21]. The conductivity of SBCCO achieves a maximum value of 34 S cm^{-1} at 850 °C. Several perovskite electrode materials with low conductivity have been reported with good electrochemical performances. For example, the maximum conductivities of $(Ba_{0.5}Sr_{0.5})_{1+x}Co_{0.8}Fe_{0.2}O_{3-\delta}$ ($0.2 \le x \le 0.6$) were about 10–50 S cm^{-1} [22]. The conductivity of the $BaCo_{0.7}Fe_{0.2}Nb_{0.1}O_{3-\delta}$ cathode was about 6.1 S cm^{-1} at 850 °C [23]. In the Conclusions section, we can find that the SBCCO cathode exhibits good electrochemical performances.

3.3. Thermal expansion behavior

Fig. 4 shows the thermal expansion curves of $SmBaCoCuO_{5+\delta}$ (SBCCO), $SmBaCo_2O_{5+\delta}$ (SBCO) and $Ce_{0.9}Gd_{0.1}O_{1.95}$ (GDC) measured from 30 to 850 °C. The parent SBCO sample has the highest TEC value of 20.24×10^{-6} K^{-1}, which is undesirable on combining in a SOFC with the GDC electrolyte that has TEC of 12.23×10^{-6} K^{-1}. The spin-state transition of the cobalt ions from low spin ($t_{2g}^6 e_g^0$) to high spin ($t_{2g}^4 e_g^2$) with increasing temperature has been reported to be the reason for the abnormally high TEC of such cobalt-based perovskite oxides [24–26]. However, the TEC value of SBCCO is 15.53×10^{-6} K^{-1}, which is ~23% lower than the TEC of the SBCO sample. The decrease in TEC with Cu doping could be attributed to the decrease in the Co content and a suppression of the spin state transitions associated with Co^{3+}. This implies that SBCCO might be more suitable as a cathode based on GDC electrolyte for IT-SOFCs.

3.4. Microstructure

Fig. 5 shows the microstructures of the fractured cells after electrochemical testing. Different SBCCO cathode (sintered at 900 °C, 950 °C and 1000 °C for 2 h) were used in the fuel cells. In general, being sintered at high-temperature increases the grain size of an electrode, which will decrease the surface area–gas solid interface then increase the polarization resistance [27]. On the other hand, due to the increase in the sintering temperature, the electrode particles adhere strongly to the electrolyte surface. Therefore, obtaining SBCCO particles with a fine microstructure and ensuring their strong adhesion to the GDC electrolyte are in a tradeoff relationship with respect to the sintering temperature. Fig. 5(a) shows that a SBCCO cathode sintered at 900 °C has an uneven distribution of the grain and poorer porosity. Fig. 5(c) shows that a SBCCO cathode sintered at 1000 °C has a much larger grain size. A SBCCO

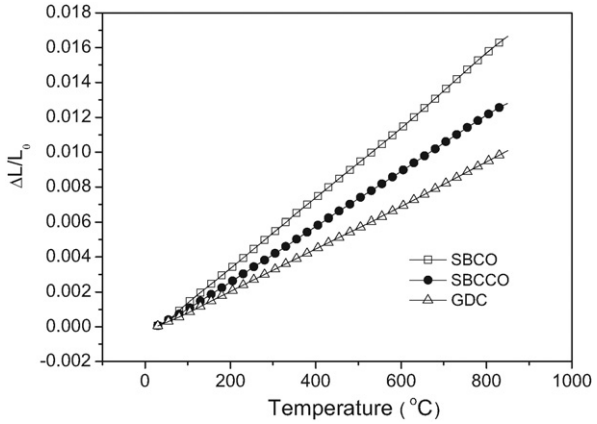

Fig. 4. Thermal expansion of different samples of SBCCO, SBCO and GDC measured in air.

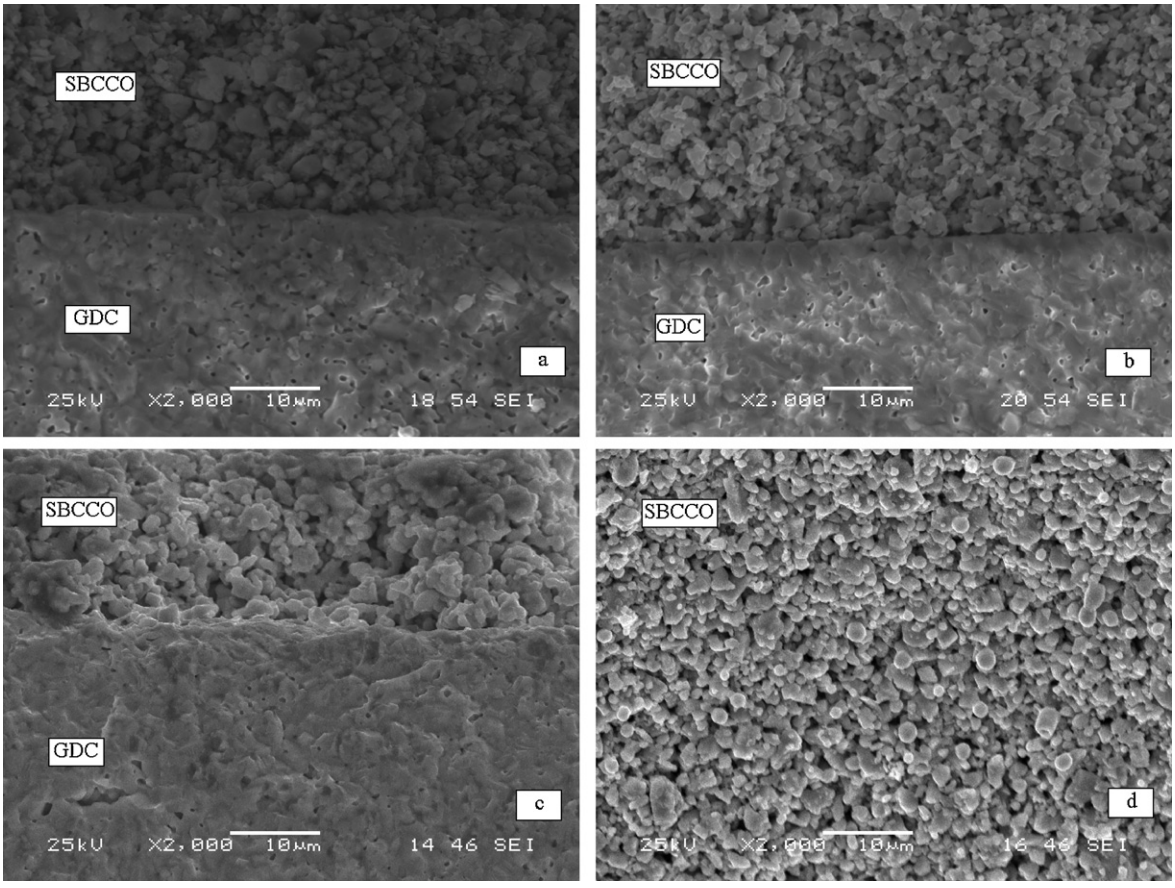

Fig. 5. Cross-sectional SEM micrographs of the fuel cell using SBCCO electrode after sintered at different temperatures: (a) 900 °C for 2 h, (b) 950 °C for 2 h and (c) 1000 °C for 2 h; (d) SEM image of surface morphology of the fuel cell using SBCCO electrode sintered at 950 °C for 2 h.

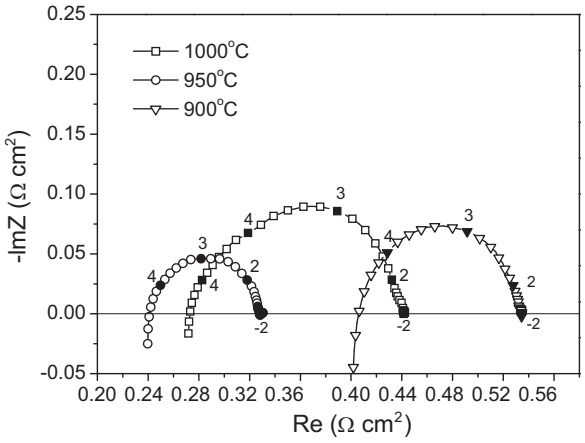

Fig. 6. Impedance spectra of SBCCO cathode sintered at 900 °C, 950 °C, 1000 °C under an open-circuit potential at 800 °C in air. The numbers in these plots correspond to logarithm of frequency.

cathode sintered at 950 °C (Fig. 5(b)) shows a smaller grain size and reasonable porosity to ensure gas diffusion. Also it appears good contact with the dense electrolyte pellet. Fig. 5(d) shows the microstructures of the SBCCO cathode surface. It presents that a fine microstructure with moderate porosity and well-necked particles had been formed.

3.5. Impedance analysis

The interfacial impedance spectra for SBCCO cathode fired at 900 °C, 950 °C and 1000 °C are shown in Fig. 6. Under an open-circuit potential at 800 °C in air, all the spectra consist of two arcs. The intercept with the real axis at high frequencies is the ohmic resistance (R_{ohm}), while the arc observed at lower frequency can be associated with the interfacial impedance between the SBCCO cathode and the GDC electrolyte. In Fig. 6, the difference of the R_{ohm} at the same measured temperature mainly attributes to the different thickness of electrolyte disk, the different length of the lead and the different contact resistance between cell and Ag mesh. The area specific resistance (ASR) value of SBCCO sintered at 950 °C on GDC electrolyte is 0.086 Ωcm^2 at 800 °C, which is much lower than the 0.168 Ωcm^2 and 0.127 Ωcm^2 for SBCCO sintered at 1000 °C and 900 °C. These results indicate that SBCCO sintered at 950 °C has the smallest interfacial resistance as well as the best electrochemical performance at open-circuit potential. And considering the SEM photo of SBCCO sintered at 950 °C (Fig. 5(b)), which showed reasonable porosity to ensure gas diffusion and good contact with the dense electrolyte pellet, we think 950 °C is the appropriate sintering temperature for this cathode.

The interfacial impedance spectra for SBCCO at temperatures ranging from 650 to 800 °C are shown in Fig. 7(a), and the equivalent circuit for the analysis of the impedance data is illustrated in Fig. 7(b). The impedance spectra consisted of two depressed semicircles. This indicates that there are at least two electrode processes corresponding to the two semi-circles during molecular oxygen reduction. According to previous workers [28,29], the semi-circle at the high frequency can be attributed to the polarization during charge transfer. On the other hand, the semi-circle at the low frequency can be attributed to oxygen adsorption/dissociation and bulk or surface oxygen diffusion process. Therefore, in the equivalent circuit, L_1 is an inductance induced by the cables; R_1 is denoted as the ohmic resistance including the electrolyte resistance and lead wires. R_2 is interpreted as the resistance of the charge transfer process through the electrode–electrolyte interface; R_3 is related to the resistance of the oxygen adsorption/desorption and bulk or

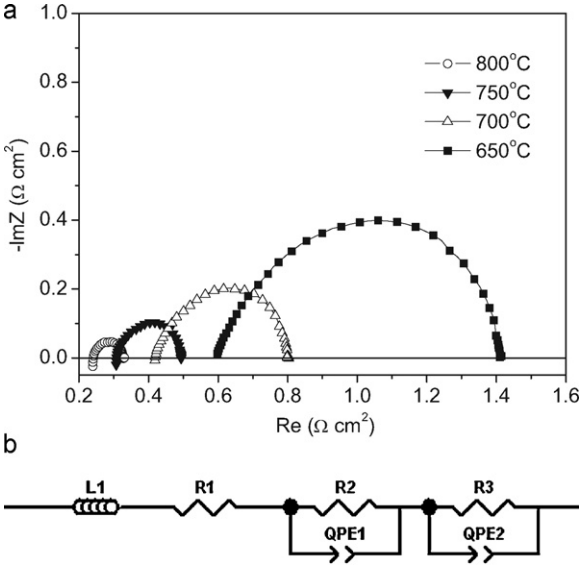

Fig. 7. (a) Impedance spectra of SBCCO cathode (sintered at 950 °C) measured at 650–800 °C. (b). Equivalent circuit model.

surface oxygen diffusion process; QPE_1 and QPE_2 correspond to the capacitance of the whole electrode.

As seen in Fig. 7(a), the ASR significantly reduces with the increasing temperature. The ASR of the SBCCO cathode is 0.813 Ω cm^2 at 650 °C, 0.382 Ω cm^2 at 700 °C, 0.185 Ω cm^2 at 750 °C and 0.086 Ω cm^2 at 800 °C, respectively. The values of ASR of SBCCO cathode are slightly higher than those of $SmBaCo_2O_{5+x}$ (SBCO) cathode reported by Shao and co-workers [30]. As described previously with the $YBaCo_{2-x}Cu_xO_{5+x}$ [31], the reason of increasing ASR of SBCCO can be understood by considering the drop of holes concentration in this system. In this double-perovskite model, the simple cubic perovskite cell is doubled along the *c* axis due to the ordering of Sm and Ba ions and along the *b* axis due to ordering of oxygen vacancies (unit cell $a_p \times 2a_p \times 2a_p$), with a_p the cubic lattice constant) [21]. Cu doping breaks the original alternation of CoO_5 pyramidal and CoO_6 octahedral planes along *a* and *b* directions in $SmBaCo_2O_{5+x}$, which hampers the hole creation, thus causing an inferior current collection and process of charge transfer for the whole cathode. However, the values of ASR for SBCCO cathode are much lower than some traditional cathodes, such as: $La_{0.6}Sr_{0.4}CoO_3$ and $Sm_{0.5}Sr_{0.5}Co_{1-x}Fe_xO_3$ [32,33]. Fig. 8 shows Arrhenius plots of the polarization resistance for SBCCO. The activation energy can be calculated from the slope of the fitted line. The activation energy of

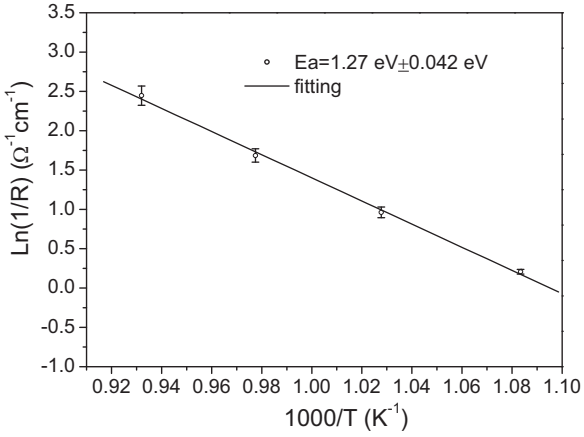

Fig. 8. Arrhenius plots of the ASR values of SBCCO cathode on GDC electrolyte.

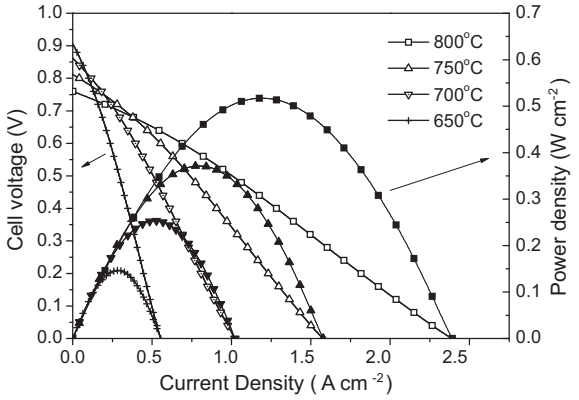

Fig. 9. Cell voltage and power density as functions of current density with SBCCO cathode.

polarization resistance is about 1.27 ± 0.042 eV. This value is close to the $SmBaCo_2O_{5+x}$ cathode reported by Zhou et al. [18].

3.6. Single-cell performance

GDC electrolyte supported fuel cells are fabricated to evaluate the performance of SBCCO electrode (sintered at 950 °C for 2 h) in real fuel cell operation conditions. Fig. 9 shows the variation of cell voltage and power density as a function of current density for the NiO-35GDC/GDC/SBCCO cell from 650 °C to 800 °C. The power density increases with increasing operating temperature. The maximum power densities of cells with the SBCCO cathode are 517, 376, and 253 mW cm^{-2} at 800, 750, and 700 °C, respectively. The performance of the cell with the single phase cathode is well compared with other cathodes, which are measured under almost the same conditions, such as: $Pr_{0.7}Sr_{0.3}Co_{0.8}Fe_{0.2}O_{3-\delta}$–$Ce_{0.85}Gd_{0.15}O_{1.925}$ [34] and $LaBaCuFeO_{5+x}$ [35]. The open-circuit voltage of this cell based on the GDC electrolyte is relatively high, which is 0.813 V at 750 °C, however, this value is still lower than theoretical value, which is mainly caused by the reduction of Ce^{4+} to Ce^{3+} at the anode atmosphere [36,37]. And the open circuit voltage (OCV) increases with the decreasing of operating temperature, indicating that the reduction of Ce^{4+} is weakened at lower temperatures [14].

4. Conclusions

Double perovskite-structure oxides $SmBaCoCuO_{5+x}$ (SBCCO) were investigated to evaluate their potential application as cathode materials for IT-SOFCs. The SBCCO oxides had a pure layered perovskite phase structure. The SBCCO cathode material also revealed a good chemical compatibility with the GDC electrolyte. The TEC value of SBCCO is 15.53×10^{-6} K^{-1}, which is ~23% lower than the TEC of the SBCO sample. The electrochemical impedance spectra revealed that SBCCO symmetrical half-cells by sintering at 950 °C had the best electrochemical performance, and the ASR of the SBCCO cathode was 0.086 Ω cm^2 at 800 °C. The maximum power densities of an electrolyte-supported cell using the SBCCO cathode were 517 mW cm^{-2} and 376 mW cm^{-2} at 800 °C and 750 °C, respectively. The above results indicated that the SBCCO cathode could be a potential candidate for IT-SOFCs.

Acknowledgments

This work was supported by the Natural Science Foundation of China (NO. 10604020), the Eleventh Five-Year Program for Science and Technology of Education Department of Jilin Province (Item No. 20100145).

References

[1] H.Y. Tu, Y. Takeda, N. Imanishi, O. Yamamoto, Solid State Ionics 117 (1999) 277–281.
[2] N.P. Brandon, S. Skinner, B.C.H. Steele, Annu. Rev. Mater. Res. 33 (2003) 183–213.
[3] B.C.H. Steele, Solid State Ionics 129 (2000) 95–110.
[4] Y. Jiang, S.Z. Wang, Y.H. Zhang, J.W. Yan, W.Z. Li, Solid State Ionics 110 (1998) 111–119.
[5] B. Morel, R. Roberge, S. Savoie, T.W. Napporn, M. Meunier, Appl. Catal. A: Gen. 323 (2007) 181–187.
[6] W. Kao, M. Lee, Y. Chang, T. Lin, C. Wang, J. Chang, J. Power Sources 195 (2010) 6468–6472.
[7] J. Yang, H. Muroyama, T. Matsui, K. Eguchi, Int. J. Hydrogen Energy 35 (2010) 10505–10512.
[8] Yi Liu, J. Alloys Compd. 477 (2009) 860–862.
[9] J.-H. Kim, A. Manthiram, J. Electrochem. Soc. 155 (2008) B385–B390.
[10] G. Kim, S. Wang, A.J. Jacobson, L. Reimus, P. Brodersen, C.A. Mims, J. Mater. Chem. 17 (2007) 2500–2505.
[11] A. Maignan, C. Martin, D. Pelloquin, N. Nguyen, B. Raveau, J. Solid State Chem. 142 (1999) 247–260.
[12] A.A. Taskin, A.N. Lavrov, Y. Ando, Appl. Phys. Lett. 86 (2005) 091910.
[13] J. Kim, Y. Kim, P.A. Connor, J.T.S. Irvine, J. Bae, W. Zhou, J. Power Sources 194 (2009) 704–711.
[14] B. Wei, Z. Lü, X. Huang, M. Liu, N. Li, W. Su, J. Power Sources 176 (2008) 1–8.
[15] Y. Ling, B. Lin, L. Zhao, X. Zhang, J. Yu, R. Peng, G. Meng, X. Liu, J. Alloys Compd. 493 (2010) 252–255.
[16] Q. Nian, L. Zhao, B. He, B. Lin, R. Peng, G. Meng, X. Liu, J. Alloys Compd. 492 (2010) 291–294.
[17] L. Cong, T. He, Y. Ji, P. Guan, Y. Huang, W. Su, J. Alloys Compd. 348 (2003) 325–331.
[18] Q. Zhou, T. He, Y. Ji, J. Power Sources 185 (2008) 754–758.
[19] A. Tarancón, D. Marrero-López, J. Peña-Martínez, J.C. Ruiz-Morales, P. Núñez, Solid State Ionics 179 (2008) 611–618.
[20] S. Streule, A. Podlesnyak, D. Sheptyakov, E. Pomjakushina, M. Stingaciu, K. Conder, M. Medarde, M.V. Patrakeev, I.A. Leonidov, V.L. Kozhevnikov, J. Mesot, Phys. Rev. B 73 (094203) (2006) 1–5.
[21] H. Gu, H. Chen, L. Gao, Y. Zheng, X. Zhu, L. Guo, Int. J. Hydrogen Energy 34 (2009) 2416–2420.
[22] W. Zhou, R. Ran, Z. Shao, W. Zhuang, J. Jia, H. Gu, W. Jin, N. Xu, Acta Mater. 56 (2008) 2687–2698.
[23] S. Lü, Y. Ji, X. Meng, G. Long, T. Wei, Y. Zhang, T. Lü, Electrochem. Solid-State Lett. 12 (6) (2009) B103–B105.
[24] M. Mori, N.M. Sammes, Solid State Ionics 146 (2002) 301–312.
[25] K. Huang, H.Y. Lee, J.B. Goodenough, J. Electrochem. Soc. 145 (1998) 3220–3227.
[26] M.A. Señarís-Rodríguez, J.B. Goodenough, J. Solid State Chem. 118 (1995) 323–336.
[27] C.J. Fu, K. Sun, N.Q. Zhang, X.B. Chen, D.R. Zhou, Electrochim. Acta 52 (2007) 4589–4594.
[28] F.H. Heuveln, H.J.M. Bouwmeester, J. Electrochem. Soc. 144 (1997) 134–137.
[29] Y.J. Leng, S.H. Chan, K.A. Khor, S.P. Jiang, Int. J. Hydrogen Energy 29 (2004) 1025–1033.
[30] K. Zhang, L. Ge, R. Ran, Z. Shao, S. Liu, Acta Mater. 56 (2008) 4876–4889.
[31] X. Zhang, H. Hao, X. Hu, Phys. B 403 (2008) 3406–3409.
[32] Z. Bi, M. Cheng, Y. Dong, H. Wu, Y. She, B. Yi, Solid State Ionics 176 (2005) 655–661.
[33] H. Lv, Y. Wu, B. Huang, B. Zhao, K. Hu, Solid State Ionics 177 (2006) 901–906.
[34] X. Meng, S. Lü, Y. Ji, T. Wei, Y. Zhang, J. Power Sources 183 (2008) 581–585.
[35] Q. Zhou, T. He, Q. He, Y. Ji, Electrochem. Commun. 11 (2009) 80–83.
[36] S.P.S. Badwal, F.T. Ciacchi, J. Drennan, Solid State Ionics 121 (1999) 253–262.
[37] M. Mogensen, N.M. Sammes, G.A. Tompsett, Solid State Ionics 129 (2000) 63–94.